03,13

Electron transfer through semiconductor-vacuum interfaces with negative and positive electron affinity: effect of jump in mass

© D.M. Kazantsev[1,2], V.S. Khoroshilov[1,2], H.E. Scheibler[1,2], V.L. Alperovich[1,2,¶]

[1] Rzhanov Institute of Semiconductor Physics, Siberian Branch, Russian Academy of Sciences, Novosibirsk, Russia
[2] Novosibirsk State University, Novosibirsk, Russia

¶ E-mail: alper_v@mail.ru

Received June 28, 2023
Revised June 28, 2023
Accepted July 10, 2023

The effect of jump in electron mass at the crystal-vacuum interface on photoemission from semiconductors is considered. In the effective mass approximation, the angular and energy dependences of the electron transmission coefficient through interfaces with jump in mass and potential steps of different signs, corresponding to negative and positive electron affinities, are considered. It is shown that due to jump in mass, there are a critical energy and a critical angle of incidence of electrons, which separate qualitatively different angular and energy dependences of the transmission coefficient, respectively. Jump in mass makes it possible for electrons to transfer (up to complete transmission) through a positive potential step with a normal component of kinetic energy below the height of the step. The calculated dependences of the emission quantum yield of thermalized electrons on the affinity value are compared with the experimental data on photoemission from *p*-GaAs(Cs,O). Possible reasons for the significant differences between the experiment and the calculation are analyzed: a complex potential profile, including the near-surface band bending in the semiconductor and the image charge potential in vacuum, scattering in the (Cs,O) layer, and the need to go beyond the effective mass approximation and to take into account full Bloch nature of electron wave functions in semiconductors.

Keywords: semiconductors, photoemission, negative electron affinity, jump in mass, effective mass approximation.

DOI: 10.61011/PSS.2023.08.56565.130

1. Introduction

Photoemission is widely used to study the electronic structure of solids [1], and also underlies the operation of a number of devices: photomultipliers, image intensifiers, sources of ultra-cold and spin-polarized electrons [2–5]. Energy and angular distributions of „ballistically“ (without scattering) emitted electrons that carry information about filled electronic states in a semiconductor are measured by photoemission spectroscopy [1]. At the same time, the energy of the radiation quanta and the kinetic energy of the electrons, as a rule, significantly exceed the work function and electron affinity. In photoemission devices, on the contrary, the emission is excited by photons with low energies close to the band gap width due to the use of photocathodes with negative effective electron affinity (NEA) $\chi^* < 0$, in which the vacuum level is below the bottom of the conduction band in the semiconductor bulk [2]. In this case, the photoemission is described in a three-step model, including: (1) photoexcitation of electrons; (2) thermalization and diffusion to the emitting surface; (3) transition across the semiconductor-vacuum interface [6]. Thus, the emitted electrons carry information mainly about the processes of relaxation of energy and momentum during transport through unoccupied states of the conduction band and during transition through the surface.

The state with NEA is achieved on the surface of highly doped *p*-GaAs by depositing (Cs,O) activation layer [3]. *p*-GaAs surfaces with relatively small ($\chi^* \approx 0.2-0.4$ eV) positive electron affinity (PEA), which can potentially be used for efficient solar energy conversion due to photon-enhanced thermionic emission are also of particular interest [7,8]. The energy band diagram of *p*-GaAs(Cs,O) surfaces with NEA and PEA, as well as the scheme of photoexcitation of electrons and their emission into vacuum are shown in Fig. 1.

Despite many years of research and applied developments, many questions of the physics of photoemission from semiconductors still remain unclear, and the parameters of the devices are still far from theoretically possible. How does the transition of an electron through the interface between a crystal and a vacuum, in other words, the transformation of a quasi-particle with a Bloch wave function into a free electron occur? How to calculate the probability of this transition correctly? What is the role of the processes of energy and momentum relaxation, as well as jump in effective mass during the transition of electrons through the interface with vacuum? It is known that jump in mass of an electron, from the effective

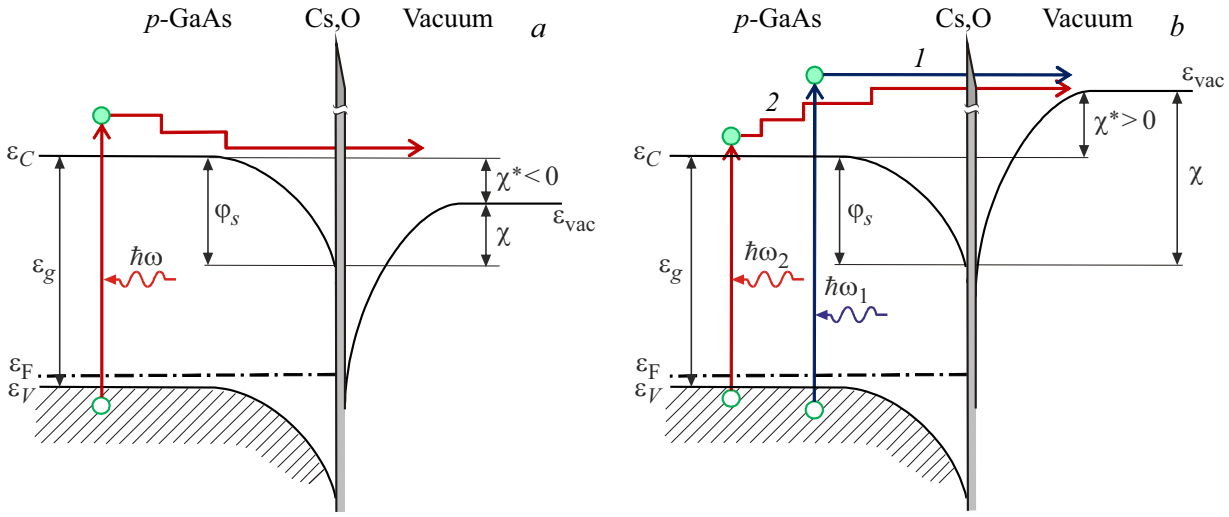

Figure 1. Energy band diagrams of the *p*-GaAs(Cs,O) surfaces with negative (*a*) and positive (*b*) electron affinity. The surface band bending φ_S in a semiconductor, the image charge potential in vacuum, the true (χ) and effective (χ^*) electron affinities, as well as a hypothetical barrier for electron escape into vacuum at the interface are shown. The arrows schematically show the interband optical transitions of electrons from the valence band to the conduction band, thermalization and diffusion to the emitting surface. The arrows in Fig. (*b*), *1* and *2* show direct photoemission and photon-enhanced thermionic emission, respectively.

mass in a semiconductor to the mass of a free electron in a vacuum, should lead to a significant narrowing of the angular distribution of the emitted electrons [2]. However, convincing experimental evidence of such a narrowing in photoemission from semiconductors with NEA has not yet been obtained, and the effect of jump in mass on emission remains a subject of discussion.

Pollard [9] reported the observation of a narrow emission cone from a *p*-GaAs(Cs,O) NEA photocathode, in agreement with the expected refraction of electron trajectories at jump in mass. Similar results were obtained in later papers [10–12]. However, the correctness of Pollard's method of measuring the narrow emission cone was questioned in a number of papers, and it was reported that wide angular distributions of electrons emitted from the *p*-GaAs(Cs,O) NEA photocathode were observed, which indicates a significant effect of electron scattering near the emitting surface [13–15]. It was experimentally shown in [16] that in case of emission from *p*-GaAs(Cs,O) NEA photocathodes, a relatively small group of electrons undergoes refraction at jump in mass, which exit into vacuum „ballistically", without scattering before emission, while most of the electrons are scattered by momentum and energy and emitted into a wide solid angle.

The problem with emission from a semiconductor with NEA is that both jump in mass and negative potential jump should lead to a narrowing of the angular distribution of the emitted electrons, so these contributions are difficult to separate in the experiment. The effect of jump in mass on the emission of electrons from semiconductors with NEA and PEA was theoretically considered in the model of the interface with potential steps of various signs in [17]. It was shown that the measurement of the angular and energy distributions of electrons emitted from semiconductors with PEA can provide a more reliable proof of the manifestation of jump in mass, compared with the state with NEA.

The mechanisms of emission from GaAs(Cs,O) were experimentally studied in [17–20] using the method of spectroscopy of the quantum efficiency of photoemission during the transition between states with NEA and PEA. Comparison of the measured spectra with the calculation did not allow proving unequivocally that jump in mass at the boundary significantly affects the emission process. At the same time, it was found that the probability of photoelectrons escaping into vacuum is significantly less than the calculation predicts. The reason for this discrepancy remains unclear.

The dependences of the coefficient of transmission through the interfaces with jump in mass on the electron energy are analyzed in this paper, in addition to the angular distributions calculated in [17]. The dependence of the quantum efficiency of the photoemission on the value of the electron affinity is calculated and compared with experimental data. The possible reasons for the differences in the calculated and experimental dependences are discussed, including the influence of the band bending in the semiconductor, the surface barrier and the image charge potential in vacuum, as well as the need to go beyond the approximation of the effective masses and take into account the Bloch nature of the electron wave functions in the semiconductor.

2. A model of the transmission of electrons through the interface with jump in mass. Angular distributions of emitted electrons

Consider the process of electron emission in a simple model of a rectangular potential step U_0 at the interface between the media *1* (semiconductor) and *2* (vacuum) with different effective electron masses m_1 and m_2. Positive ($U_0 > 0$) and negative ($U_0 < 0$) potential steps correspond to the states of the surface with positive and negative effective electron affinity χ^*. The energy conservation law relates the energies of incident (ε_1) and transferred (ε_2) electrons: $\varepsilon_2 = \varepsilon_1 - U_0$. For parabolic dispersion laws, $\varepsilon_1 = m_1 v_1^2/2$, $\varepsilon_2 = m_2 v_2^2/2$, where v_1 and v_2 are the corresponding electron velocities. Assuming that the tangential component of the momentum is preserved during emission, we obtain a relationship between the angles of incidence θ_1 and refraction θ_2:

$$\frac{\sin\theta_1}{\sin\theta_2} = \sqrt{\frac{m_2(\varepsilon_1 - U_0)}{m_1\varepsilon_1}}. \quad (1)$$

Boundary conditions for the envelopes of wave functions preserving the electron flux were used to calculate the coefficients of quantum mechanical reflection and transmission in the effective mass approximation; the Bloch amplitudes were considered constant [21,22]. A simple and widely used form of these conditions consists in matching, at the boundary, the envelopes of the wave functions $\psi_1 = \psi_2$ and their first derivatives in the direction of the normal to the surface z, normalized by the values of the effective masses [23]:

$$\frac{1}{m_1}\frac{\partial\psi_1}{\partial z} = \frac{1}{m_2}\frac{\partial\psi_2}{\partial z}. \quad (2)$$

For such boundary conditions, the reflection coefficient R and the transmission coefficient T of the electron flux are compactly expressed in terms of the normal components of the velocities of incident v_{1z} and transferred v_{2z} electrons:

$$R = \frac{(v_{1z} - v_{2z})^2}{(v_{1z} + v_{2z})^2}, \quad (3)$$

$$T = \frac{4v_{1z}v_{2z}}{(v_{1z} + v_{2z})^2}. \quad (4)$$

From these relations it can be seen that the zero reflection $R = 0$ and the total transmission $T = 1$ correspond to the equality of the normal components of the velocities of the incident and transmitted electrons $v_{1z} = v_{2z}$. In turn, the values v_{1z} and v_{2z} can be expressed in terms of ε_1, θ_1, U_0, m_1 and m_2:

$$v_{1z} = \sqrt{\frac{2\varepsilon_1}{m_1}}\cos\theta_1, \quad (5)$$

$$v_{2z} = \sqrt{\frac{2(\varepsilon_1 - U_0)}{m_2}}\cos\theta_2 = \sqrt{\frac{2\left(\varepsilon_1 - U_0 - (m_1/m_2)\varepsilon_1\sin^2\theta_1\right)}{m_2}}. \quad (6)$$

It should be noted that when substituting (5) and (6) into (3) and (4), the resulting expressions for reflection and transmission coefficients do not depend on m_1 and m_2 separately, but only on the mass ratio $\mu = m_1/m_2$. In all calculations below, the value of m_2 was assumed to be equal to the mass of the free electron.

Using the expressions (3)–(6), in the work [17], the dependences of the transmission coefficient on the angle of incidence $T(\theta_1)$ at different electron energies ε_1 were analyzed for the cases of positive and negative potential steps, without jump and with jump in mass at the interface. It was shown that in the absence of a potential step ($U_0 = 0$), the relations (1) and (3), (4) do not depend on the electron energy, and these relations coincide with the Snell's law and Fresnel formulas for *p*-polarized light, respectively, with the replacement of the ratio of refractive indices by the root of the mass ratio. Similarly to Brewster's phenomenon in optics, at $U_0 = 0$, the electron reflection coefficient from the interface is zero if the angle of incidence satisfies the relation $\tan(\theta_B) = \sqrt{m_2/m_1}$.

For the cases of potential steps of both signs, due to jump in mass at the boundary, there are critical energies that separate regions with qualitatively different angular dependencies of the transmission coefficient $T(\theta_1)$ [17]. In the case $U_0 > 0$ corresponding to the state with PEA, the critical energy of the emitted electrons ε_{2c} corresponds to the intersection point of the dispersion laws in a semiconductor and in a vacuum, for which all the components of the momentum are preserved during emission, and there is no refraction of the electron trajectories due to compensation of the contributions of the positive potential step and jump in mass. At energies higher than the critical $\varepsilon_2 > \varepsilon_{2c}$, refraction at jump in mass prevails, which narrows the angular distribution of the emitted electrons, and at $\varepsilon_2 < \varepsilon_{2c}$ — refraction at the positive potential step, which broadens the angular distribution. In this regard, an experiment was proposed to clarify the role of jump in mass at the semiconductor–vacuum interface by the angular distributions of electrons emitted from the semiconductor with the state of PEA.

The angular distribution functions of the emitted electrons $N_2(\theta_2)$ were calculated in [17], while the results of the proposed experiment should be compared with the calculated electron flux. In this paper we calculated the angular dependences of the electron flux $J_2(\theta_2)$ emitted from a semiconductor with PEA ($U_0 > 0$) with different energies ε_2 in the absence of jump in mass and for jump in mass $\mu = m_1/m_2 = 0.067$ corresponding to effective mass in GaAs. It was assumed that the electrons inside the semiconductor have a Maxwell-Boltzmann velocity distribution. The calculated dependencies are shown in Fig. 2.

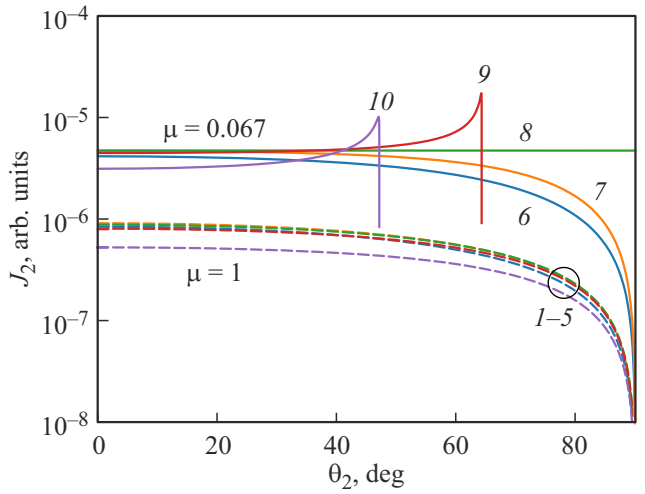

Figure 2. Distributions of the flux of emitted electrons J_2 (per unit of solid angle) along the emission angle θ_2 calculated for a positive potential step $U_0 = 0.4$ eV in the absence of jump in mass $\mu = 1$ (dashed lines *1–5*) and for jump in mass $\mu = 0.067$ (solid lines *6–10*) for various energies of emitted electrons ε_2: 0.014 eV (lines *1* and *6*); 0.021 eV (lines *2* and *7*); 0.029 eV (lines *3* and *8*, critical energy $\varepsilon_2 = \varepsilon_{2c}$ for $\mu = 0.067$); 0.036 eV (lines *4* and *9*); 0.057 eV (lines *5* and *10*).

It can be seen that in the absence of jump in mass $\mu = 1$, the flux $J_2(\theta_2)$ decreases with an increase in the emission angle over the entire energy range (dashed curves *1–5*) due to an increase in the quantum mechanical reflection of electrons from the potential step. The curves *1–5* lie close to each other in a relatively narrow band, due to the combined effect of two multidirectional factors: on the one hand, an increase in energy reduces the reflection of electrons from the potential step; on the other hand, the number of electrons decreases with energy according to the Maxwell–Boltzmann distribution.

The angular dependences of the flux of emitted electrons $J_2(\theta_2)$ are shown in Fig. 2 by solid lines *6–10* for jump in mass $\mu = 0.067$. For the critical electron energy $\varepsilon_2 = \varepsilon_{2c}$ (line *8*) the electron flux does not depend on the emission angle θ_2 due to the absence of refraction. Electrons emit in the entire angle range from 0 to 90° at energies below the critical, and the flux $J_2(\theta_2)$ monotonically decreases to zero with increasing angle θ_2, similar to the case of $\mu = 1$, due to the prevailing refraction at the positive potential step. On the contrary, the area of emission angles is limited at energies above the critical one due to refraction at jump in mass, and the flux $J_2(\theta_2)$ increases with the increase of the emission angle.

Thus, for a positive potential step $U_0 > 0$ and jump in mass $\mu < 1$, the critical energy separates regions with qualitatively different angular distributions of emitted electrons. As a consequence, for the case of PEA, the experimental measurement of the angular distributions of emitted electrons can indicate the significance of the refraction effect on jump in mass when electrons pass through the semiconductor–vacuum interface, due to the energy separation between decreasing and growing angular distributions. It should be noted that for the GaAs-vacuum interface, the critical energy of the emitted electrons $\varepsilon_{2c} = U_0\mu/(1-\mu)$ is relatively small ($\sim 15-30$ meV for $U_0 \approx 0.2-0.4$ eV), therefore, an analyzer with a very high energy and angular resolution is needed. Such analyzers were not available until the authors of [24] developed a three-dimensional momentum and energy analyzer, which allows, in principle, measuring the angular distributions of electrons with the accuracy required to clarify the role of jump in mass.

3. Energy dependences of transmission coefficient at the interfaces with jump in electron mass

This section presents the dependences of the transmission coefficient T through the interfaces with jump in mass and potential steps of various signs on the energy of incident electrons. These results complement the angular dependences calculated for various energies [17] and clearly illustrate the nontrivial effects caused by jump in mass. Fig. 3 shows the dependencies of the transmission coefficient T on the normal to the surface component of the kinetic energy of incident electrons $\varepsilon_{1\perp}$, normalized to the height of the potential step U_0, at different angles of incidence, in the case of $U_0 > 0$ (corresponding to positive affinity), for jump in mass $\mu = 0.25$, close to the effective electron mass in GaN (curves *1–4*), and in the absence of jump in mass $\mu = 1$ (curve *5*). Without

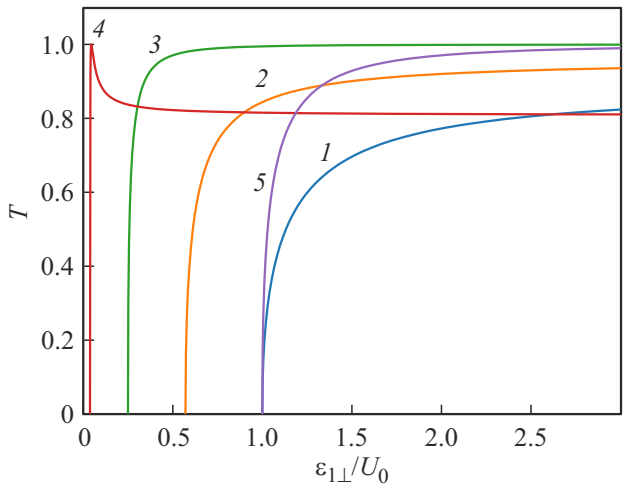

Figure 3. Dependence of the transmission coefficient T on the normal component of the kinetic energy of incident electrons, normalized by the value of the potential step $\delta_\perp = \varepsilon_{1\perp}/U_0$ at the interface of media with jump in mass $\mu = 0.25$ (curves *1–4*), for various angles of incidence: *1* — $\theta_1 = 0°$; *2* —45°; *3* — 63° (critical angle $\theta_1 = \theta_c$); *4* — 80°. Curve *5* shows a case without jump in mass $\mu = 1$, for which the function $T(\delta_\perp)$ does not depend on the angle of incidence.

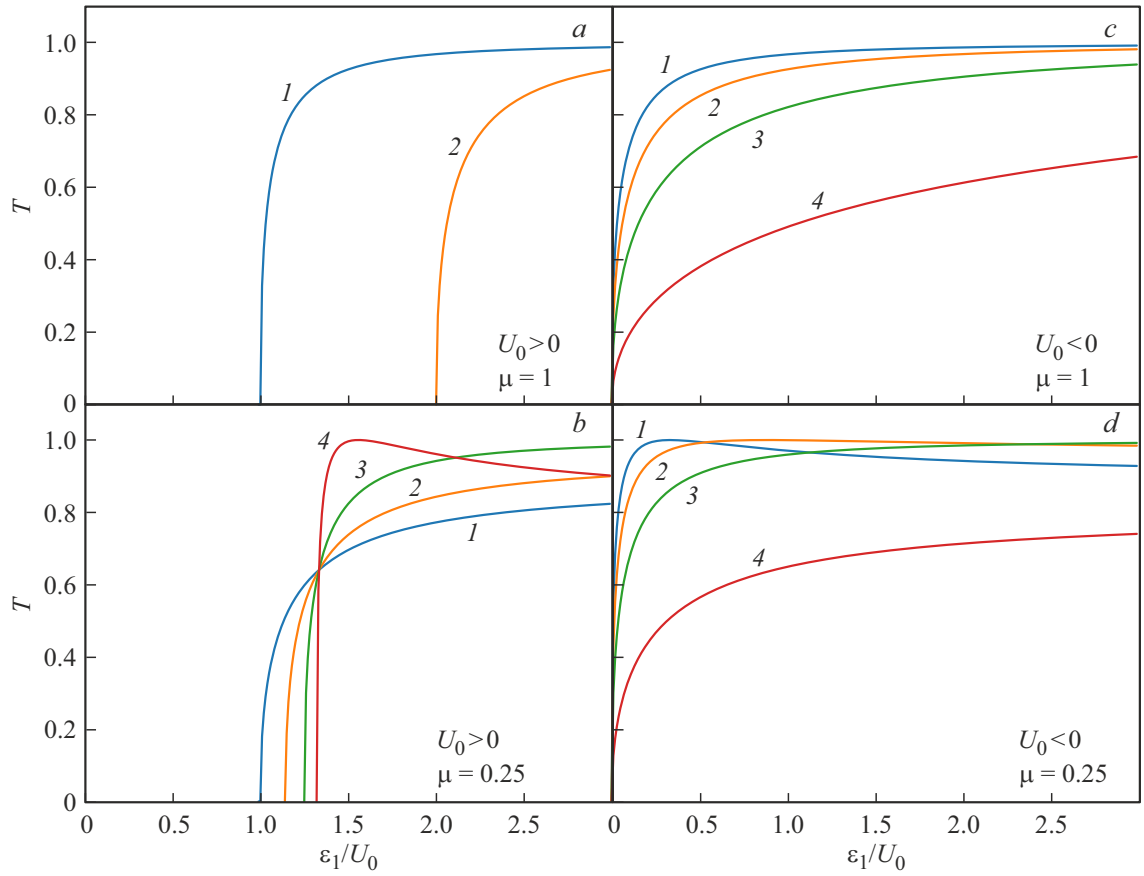

Figure 4. Dependencies of the transmission coefficient T on the total kinetic energy of incident electrons normalized by the absolute value of the potential step $\delta = \varepsilon_1/|U_0|$ calculated for $U_0 > 0$ (a, b) and $U_0 < 0$ (c, d), for jump in mass $\mu = 1$ (a, c) and $\mu = 0.25$ (b, d) at different angles of incidence: *1* — $\theta_1 = 0°$; *2* — 45°; *3* — critical angle $\theta_1 = \theta_c \approx 63°$; *4* — 80°.

jump in mass $\mu = 1$, only electrons with a normal kinetic energy component exceeding the height of the barrier $\varepsilon_{1\perp} > U_0$ can pass through the interface; at the same time, the transmission coefficient monotonically increases with increasing $\varepsilon_{1\perp}$ from zero at the threshold $\varepsilon_{1\perp} = U_0$ to $T = 1$ in the limit of high energies and does not depend on the angle of incidence.

In the case of jump in mass $\mu < 1$, with a normal incidence $(\theta_1 = 0°)$, the function $T(\varepsilon_{1\perp})$ also monotonically increases with the growth of $\varepsilon_{1\perp}$, but saturation occurs at $T < 1$ (curve *1*). Comparison of the curves *1* and *5* shows that the transmission coefficient is less than in the case of $\mu = 1$ at any energy due to the additional reflection of electrons caused by jump in mass. It can be seen that with a deviation from the normal incidence $\theta_1 > 0°$ (curves *2–4*), the threshold of transmission shifts towards lower energies $\varepsilon_{1\perp}$. Thus, the electrons with a normal kinetic energy component, lower than the barrier height, can transfer through the interface due to jump in mass because of the conversion of the tangential energy component to the normal one. In addition, the shape of the dependencies $T(\varepsilon_{1\perp})$ differs significantly for the angles of incidence θ_1, smaller and larger critical angle θ_c satisfying the condition $\tan(\theta_c) = \sqrt{m_2/m_1}$. Note that the critical angle coincides with the Brewster angle $\theta_c = \theta_B$, for which a complete transmission of $T = 1$ takes place in the case of $U_0 = 0$. For $\theta_1 \leq \theta_c$, the function $T(\varepsilon_{1\perp})$ is monotonic, as in the absence of jump in mass, and it becomes non-monotonic for $\theta_1 > \theta_c$: T increases at low energies $\varepsilon_{1\perp}$, passes through the point of total electron transmission $T = 1$ at an energy corresponding to the coincidence of normal velocity components $v_{1z} = v_{2z}$ (see formula (3)), and again decreases to some value $T < 1$.

It is convenient to use the dependences of the transmission coefficient on the total energy of incident electrons $T(\varepsilon_1)$ to describe photoemission experiments. The dependences of T on the energy normalized by the absolute value of the potential step $\delta = \varepsilon_1/|U_0|$ are shown in Fig. 4 for the cases of $U_0 > 0$ (Fig. 4, *a, b*) and $U_0 < 0$ (Fig. 4, *c, d*), and also $\mu = 1$ (Fig. 4, *a, c*) and $\mu = 0.25$ (Fig. 4, *b, d*). For a positive step $U_0 > 0$, in the absence of jump in mass $\mu = 1$ (Fig. 4, *a*), the value of T monotonically increases with energy, starting from the threshold, which is determined by a condition for the normal energy component $\varepsilon_1 = U_0/\cos^2\theta_1$. This threshold shifts to higher energies with increasing angle of incidence of θ_1 and tends to infinity at $\theta_1 \to 90°$.

The dependencies of $T(\varepsilon_1)$ change qualitatively at $\mu < 1$ (Fig. 4, *b*): the transmission threshold still increases with the angle of incidence θ_1, but remains finite at $\theta_1 \to 90^\circ$ due to the effect of converting the tangential component of kinetic energy to normal at the interface with jump in mass. It can be seen that all dependencies intersect at one point, at a critical energy $\varepsilon_{1c} = U_0/(1-\mu)$, for which there is no refraction of electron trajectories, and the reflection and transmission coefficients do not depend on the angle of incidence. Note that the transmission coefficient remains less than one for critical energy, despite the absence of refraction. In this case, the partial reflection of the electron from the interface occurs due to the discontinuity of the derivative of the wave function due to jump in mass. As in the case of dependencies $T(\varepsilon_{1\perp})$ (Fig. 3), the critical angle separates the regions of monotonic (at $\theta_1 < \theta_c$) and non-monotonic ($\theta_1 > \theta_c$) energy dependencies $T(\varepsilon_1)$. Thus, in the case of a positive step, jump in mass contributes to a decrease in the threshold energy of electron transfer through the interface, as well as an increase in the transmission coefficient up to $T = 1$ at angles of incidence greater than the critical one.

There is also a quantum mechanical reflection of electrons for the negative step $U_0 < 0$, although the threshold energy of transfer is zero (Fig. 4, *c, d*). In the absence of jump in mass $\mu = 1$, the transmission coefficient monotonically increases with the energy ε_1 for all angles of incidence θ_1 and decreases with θ_1 (Fig. 4, *c*). For the boundary with jump in mass $\mu < 1$ (Fig. 4, *d*), as in the case of $U_0 > 0$, the critical angle θ_c separates the regions of monotonic and non-monotonic dependencies $T(\varepsilon_1)$. However, unlike $U_0 > 0$, at $U_0 < 0$, non-monotonic dependencies $T(\varepsilon_1)$ with a maximum corresponding to the complete transfer $T = 1$ are observed at angles less than the critical $\theta_1 < \theta_c$.

4. Dependence of the quantum efficiency of photoemission on effective electron affinity

It can be seen from the comparison of Fig. 4, *c* and 4, *d* that in the case of a negative potential step $U_0 < 0$, jump in mass $\mu < 1$ increases the probability of electron transfer through the interface. The estimation of the „optimal“ value U_0, at which the maximum quantum efficiency of photoemission of thermalized electrons is achieved, can be performed from the condition that for electrons with a normal kinetic energy component equal to $k_B T_0/2$ (k_B is the Boltzmann constant, $T_0 = 300$ K is the room temperature), transmission coefficient at normal incidence is maximal and equal to one. For $\mu = 0.067$, this estimate yields $U_0 \approx -0.18$ eV, which is close to typical values of negative effective electron affinity in high-efficiency *p*-GaAs(Cs,O) photocathodes [2,3,25]. Therefore it can be assumed that jump in mass contributes to an increase in the quantum efficiency of NEA photocathodes.

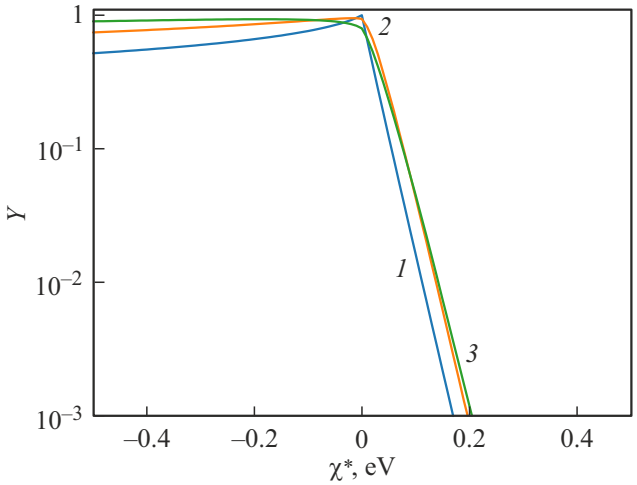

Figure 5. Dependences of the photoemission quantum efficiency Y of thermalized electrons from a semiconductor on the value of the effective electron affinity χ^* calculated at room temperature $T_0 = 300$ K for various electron jumps in mass: *1* — $\mu = 1$; *2* — 0.25; *3* — 0.067.

To assess the significance of this contribution we calculated the photoemission quantum efficiency Y of thermalized electrons from a semiconductor into vacuum in a model with jump in mass μ and a potential step height U_0 equal to the value of the effective electron affinity of the surface χ^*. The quantum efficiency Y was defined as the ratio of the flux of emitted electrons, taking into account the transmission coefficient $T(v_{1z}, \chi^*)$, to the total flux of electrons incident on the surface from the bulk of the semiconductor

$$Y(\chi^*) = \frac{\int\limits_{v_{1z}>0} v_{1z} f_B(\varepsilon_1) T(v_{1z}, \chi^*) d^3 v_1}{\int\limits_{v_{1z}>0} v_{1z} f_B(\varepsilon_1) d^3 v_1}, \qquad (7)$$

where $f_B(\varepsilon_1)$ is the Boltzmann distribution. The dependence $Y(\chi^*)$ is shown in Fig. 5 for different values of jump in electron mass. It can be seen that in the region of PEA $\chi^* > 0$, the quantum efficiency decreases exponentially with increasing affinity due to the Boltzmann decrease in the number of electrons that can overcome the surface potential barrier and exit into vacuum.

It can be seen from Fig. 5 that jump in electron mass leads to an increase in the quantum efficiency for both large positive and large negative effective affinities $|\chi^*| > k_B T_0$. With positive affinity, the increase of Y is explained by the possibility for electrons with a normal kinetic energy component below the vacuum level $\varepsilon_\perp < \chi^*$ to overcome the surface barrier by converting the tangential energy component to normal. In case of a negative affinity, an increase of Y is associated with an increase in the transmission coefficient due to a better agreement of the normal components of electron velocities in the semiconductor $v_{1z} \sim \sqrt{k_B T_0/m_1}$ and vacuum $v_{2z} \sim \sqrt{2\chi^*/m_2}$ at $m_1 < m_2$.

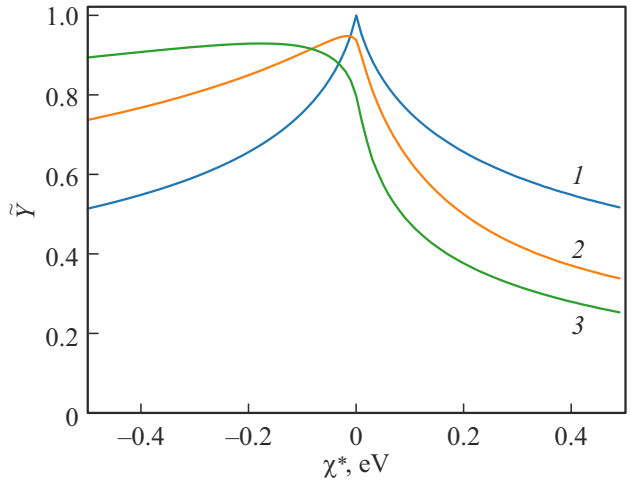

Figure 6. The quantum efficiency of the photoemission $\tilde{Y}(\chi^*)$, redefined by normalization to the flux of incident electrons that are allowed to exit the semiconductor into vacuum by conservation laws, depending on the electron affinity χ^*, calculated for the same values of jump in mass as in Fig. 5: *1* — $\mu = 1$; *2* — 0.25; *3* — 0.067.

The effect of jump in mass on the quantum yield turned out to be more complex for small affinity values $|\chi^*| \leq k_B T_0$. The behavior in this area is explained by Fig. 6. This figure shows the dependences of the quantum efficiency $\tilde{Y}(\chi^*)$ which was calculated as the flux of electrons in a vacuum, normalized not to the total flux incident on the surface, but only to the part of the flux consisting of electrons that can escape into vacuum according to the energy and momentum conservation laws. Thus, the dependences $\tilde{Y}(\chi^*)$ reflect only the effect of potential steps and jump in mass on the quantum-mechanical reflection and transfer of electrons, while the Boltzmann exponential dependence of the emitted flux on affinity at $\chi^* > 0$ was excluded. As a result, the shape and order of the curves in the area of the PEA ($\chi^* > 0$) have changed compared to Fig. 5: it can be seen that jump in mass not increases, but decreases $\tilde{Y}(\chi^*)$. The reason is that, in contrast to the case of $\chi^* < 0$, at $\chi^* > 0$, jump in mass $\mu < 1$ increases the mismatch of the normal components of the velocities of incident and transmitted electrons and, thus, increases reflection and reduces transmission.

It is interesting to note that in the absence of jump in mass $\mu = 1$, the function $\tilde{Y}(\chi^*)$ is symmetric with respect to the affinity sign and has a „beak-like“ feature near zero affinity. At point $\chi^* = 0$, the transmission is $\tilde{Y} = 1$ (the environments *1* and *2* are equivalent, there is no interface). The decline of $\tilde{Y}$ with an increase of χ^* is determined by the mismatch of the normal components of the velocities of incident and transmitted electrons due to the action of a potential step. The symmetry of the function $\tilde{Y}(\chi^*)$ with respect to the sign change of χ^* is due to the symmetry of the formulas (3), (4) for the reflection and transmission coefficients with respect to the velocity permutation v_{1z} and v_{2z}. The singularity is smoothed out and the dependence $\tilde{Y}(\chi^*)$ becomes asymmetric at $\mu < 1$. The resulting smooth maximal is shifted to the NEA region so that the values of the quantum efficiency $\tilde{Y}$ at negative values of effective affinity are greater than at the same modulo positive affinity values. The maximum position of $\chi^* \approx -0.175$ eV is close to the estimate made above at $\mu = 0.067$, as well as to the optimal value of the effective electron affinity at which the maximal quantum efficiencies of GaAs(Cs,O) photocathodes [25] are achieved.

The calculation results shown in Fig. 6 suggest that jump in mass at the semiconductor-vacuum interface can make a significant contribution to the quantum efficiency of NEA photocathodes. To test this assumption, we compared the calculation with the experimental dependence of $Y(\chi^*)$, measured in [25] when activating *p*-GaAs(Cs,O) NEA-photocathode (Fig. 7). The affinity value $\chi^* \approx -0.15$ eV, at which the maximum quantum efficiency is observed on the experimental dependence, is close to the maximum position for the curve calculated in a simple model of a potential step and jump in mass. However, it can be seen from Fig. 7 that this calculation (solid line) does not describe the magnitude and shape of the measured dependence $Y(\chi^*)$. One of the possible reasons for the discrepancy between the experiment and the calculation is the scattering of electrons in the activation Cs–O layer [26]. The dashed line on Fig. 7 shows a calculation in which this scattering is taken into account semi-empirically by multiplying by an exponential factor $0.4\exp(-d/\lambda)$, where the thickness of the (Cs,O) layer d increases during activation from 0 to ~ 3 nm [25], the electron free path length $\lambda \approx 2$ nm served as a fitting parameter.

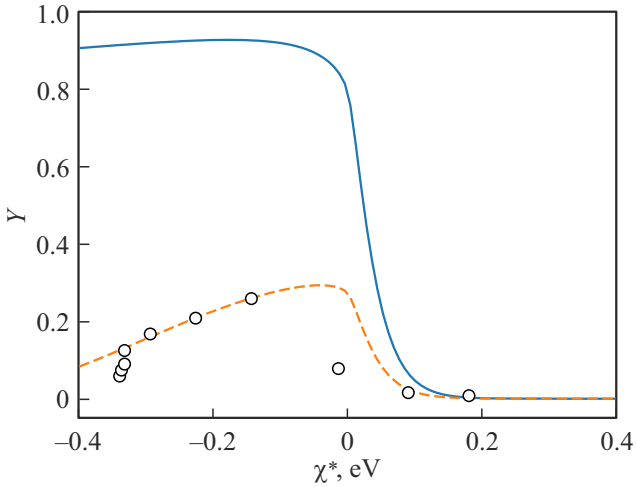

Figure 7. Dependences of the quantum efficiency of photoemission Y on the value of the effective electron affinity χ^* on the GaAs(Cs,O) surface: points — experimental data from the work [25]; solid line — calculation in the model of a potential step height χ^* with jump in mass $\mu = 0.067$; dashed line — calculation in which additionally, electron scattering in the (Cs,O) layer is taken into account (see text).

A multiplier of 0.4, taking into account, among other things, the reflection of light and the finite diffusion length of photoelectrons, was introduced to coordinate the quantum efficiency with the experiment. It can be seen that such a calculation made it possible to provide a good description of the experiment in the area of $\chi^* \leq -0.15$ eV, however, at $\chi* > -0.15$ eV there remains a significant discrepancy. It should be noted, however, that the value obtained by fitting $\lambda \approx 2$ nm is at least an order of magnitude less than expected from the known universal energy dependence of the electron path length for energies ≤ 1 eV [1].

A significant discrepancy was also found between experimental and calculated values of the quantum efficiency of photoemission and photon-enhanced thermionic emission in [19,20] when describing the spectra of the quantum efficiency of photoemission from p-GaAs(Cs,O) photocathodes measured in the region of zero and a small positive effective affinity $\chi^* \leq 0.4$ eV. The discrepancy was expressed in the fact that in order to be consistent with the experiment, the spectral contributions of hot and thermalized electrons, calculated taking into account quantum mechanical reflection, had to be multiplied by additional dimensionless coefficients — P_h and P_t, i.e. „escape probabilities“ which turned out to be significantly less than one: $P_h, P_t \leq 0.1-0.2$. Small probabilities of electron transfer into vacuum were also observed on Cs/GaAs surfaces with submonolayer cesium coverages and a small positive affinity $\chi^* \leq 0.3$ eV [18]. In a number of papers, it was argued that the low probability of transfer into vacuum with a single collision of an electron with the surface of a semiconductor is also characteristic of p-GaAs(Cs,O) with negative effective affinity $\chi^* < 0$ [27,28]. At the same time, according to [27], a relatively large (~ 0.5) quantum yield of NEA-photocathodes is provided by the capture of electrons to quantum-dimensional states localized in the band bending region, and by „multiple collisions“ with the surface during the lifetime at these states.

Thus, for GaAs surfaces with both negative and positive effective affinity, the probability of reflection of an electron with sufficient energy to escape into vacuum is significantly greater, and the transmission probability is significantly less than predicted by the calculation taking into account the over-barrier reflection from the potential step and jump in effective mass. In a number of works it was assumed that the reason for the large electron reflection coefficient at the GaAs(Cs,O)-vacuum boundary is the presence of some tunnel-transparent potential barrier caused, in particular, by the activating (Cs,O) layer [29]. This narrow hypothetical barrier, with a thickness of several monolayers, is schematically shown near the semiconductor-vacuum interface in Fig. 1. It is clear that by varying the thickness and height of this barrier, any values of reflection and transmission coefficients can be easily explained. It is possible that the characteristic attenuation length of the emitted electron flux $\lambda \approx 2$ nm obtained from the fitting of the dependence $Y(\chi^*)$ (Fig. 7) is due to tunneling through the barrier caused by the (Cs,O) layer. Nevertheless, we do not know reliable experimental or theoretical justifications for the existence of such a barrier on the Cs/GaAs surface with submonolayer cesium coatings. It is possible that an important role in limiting the probability of emission into vacuum is played by electron scattering near the surface on the roughness of the relief [30], as well as on fluctuations in the potential created by charged surface states and acceptors in the band bending region.

Another possible reason for the discrepancy between the experiment and the calculation is that a simple model of a rectangular potential step does not take into account the real band diagram of the semiconductor−vacuum interface (Fig. 1). However, our preliminary calculation of the probabilities of reflection and transmission of electrons, taking into account the surface band bending in a semiconductor and the image charge potential in vacuum [31], showed that, in the current range of values of band bending and p-GaAs doping levels, these factors do not lead to a significant change in the dependency $Y(\chi^*)$.

A possible fundamental reason for the low probability of electron emission into vacuum is that the calculation of the electron transfer through the boundary must be carried out not in the effective mass approximation, with boundary conditions on the envelopes of wave functions, but taking into account the complete Bloch functions of electrons in the crystal. This question was considered theoretically for photoemission from metals [32,33], and also from semiconductors [28]. In particular, numerical calculations carried out in [28], taking into account the Bloch nature of wave functions, predict significant differences in the magnitude of the quantum yield of photoemission for different crystallographic orientations of GaAs(Cs,O) surfaces. Nevertheless, numerical calculations do not provide a simple physical explanation of the reasons for the small probability of electron transmission through the boundary. The transmission of electrons through a heterojunction was considered in [34] in a simple one-dimensional tight-binding model. It turned out that the electron transmission coefficient significantly depends on the microscopic parameters of the heterojunction, and as a rule, is less than calculated in the effective mass approximation.

In our opinion, a qualitative explanation of the smallness of the emission probability can also be given in the nearly free electron model. In this model the allowed energy bands separated by the forbidden gaps are formed on the basis of the parabolic dispersion law of the free electron, translated to the vectors of the reciprocal lattice $\mathbf{G}$. A photoelectron with sufficient energy can emit with the tangential components of the momentum $\mathbf{p}_t$ in vacuum equal to the tangential components of the quasi-momentum in various Brillouin zones $\mathbf{p}_t = \mathbf{k}_t + \mathbf{G}_t$, where $\mathbf{k}_t$ is the quasi-momentum of the electron in the first Brillouin zone. In other words, during emission, electron diffraction occurs on the crystal. The most intense diffraction beam, apparently, corresponds to the emission from the Brillouin zone in which the electron state is close to the original parabolic dispersion law of a free electron in vacuum. Indeed, for such a state, the Bloch

amplitude weakly depends on the coordinate in comparison with equivalent states in other Brillouin zones, and the wave function of an electron in a crystal is close to a plane wave in a vacuum. It can be said that the emission from such a state corresponds to the zero order of diffraction. As a rule, due to the large value of the internal potential [35], the emission corresponding to the zero diffraction order originates from the Brillouin zone with a large quasi-momentum.

When emitted under the action of photons with high energy (as in the photoelectron spectroscopy method [1]), the electron energy is sufficient to escape into a vacuum with a large momentum in the zero diffraction order. On the contrary, emission from semiconductors with NEA occurs at low photon energies, near the band gap. In this case, the energy conservation law permits the emission only from the first Brillouin zone with a small quasi-momentum. Such emission corresponds to a non-zero diffraction order, so its probability should be smaller. In other words, this probability is less due to the fact that the wave function is „loaded" with Bloch amplitude, rapidly oscillating in space, and this explains the smallness of the experimentally observed probability of photoelectrons escaping from semiconductors into vacuum.

5. Conclusion

The paper considers the effect of an electron jump in mass at the crystal-vacuum interface on photoemission from semiconductors with negative and positive electron affinity. The angular and energy dependences of the electron transmission coefficient through the interfaces with jump in mass $\mu = m_1/m_2$ and potential steps U_0 of various signs are calculated in the effective mass approximation, which correspond to the cases of positive $(U_0 > 0)$ and negative $(U_0 < 0)$ affinities. It was shown that transmission of electrons with a normal kinetic energy component lower than the step height through the boundary is possible at $\mu < 1$ and $U_0 > 0$ due to the transformation of the tangential energy component into the normal one. It was found that the critical angle θ_c separates qualitatively different, monotonic and non-monotonic dependences of the electron transmission coefficient on the energy $T(\varepsilon)$, and in the second case, the dependence $T(\varepsilon)$ passes through the maximum of the complete transmission of $T = 1$, corresponding to the coincidence of normal components of electron velocities in the crystal and vacuum. Similarly, the critical energies separate the monotonic and non-monotonic dependences of the transmission coefficient on the angle of incidence for the steps of both signs, and for $U_0 > 0$ this separation is significantly stronger than for $U_0 < 0$ [17].

The dependences of the quantum efficiency of thermalized electrons photoemission from a semiconductor into vacuum on the magnitude and sign of the effective affinity $Y(\chi^*)$ for different values of jump in mass at the interface are calculated. Jump in mass increases the quantum efficiency of emission for actual values of negative affinity $\chi^* \sim -(0.1-0.3)$ eV. The calculation is compared with the experimental dependence $Y(\chi^*)$ for the surface *p*-GaAs(Cs,O). The possible reasons for the significant differences in the shape and amplitude of the calculated dependences $Y(\chi^*)$ from the experiment are analyzed: a potential barrier at the interface, a complex potential profile including surface band bending in a semiconductor and the image charge potential in vacuum, scattering in the activating (Cs,O) layer. The necessity of taking into account the Bloch nature of wave functions in a semiconductor is also discussed to explain the smallness of the probability of an electron escaping into vacuum in comparison with the calculated one in the effective mass approximation. A qualitative explanation of this smallness is proposed, based on the diffraction of electrons on the crystal lattice during emission into vacuum and the influence of Bloch amplitudes on the probability of emission.

Acknowledgments

The authors would like to thank A.G. Zhuravlev, L.S. Braginsky, M.V. Entin, L.D. Shvartsman, A.V. Nenashev, V.A. Tkachenko and S.A. Tarasenko for useful discussions.

Funding

The study was supported by the Russian Science Foundation grant No. 23-72-30003, https://rscf.ru/en/project/23-72-30003/

Conflict of interest

The authors declare that they have no conflict of interest.

References

[1] A. Damascelli. Physica Scripta **109**, 61 (2004).
[2] R.L. Bell. Negative Electron Affinity Devices. Clarendon, Oxford. (1973). 148 p.
[3] V.V. Bakin, A.A. Pakhnevich, A.G. Zhuravlev, A.N. Shornikov, I.O. Akhundov, O.E. Tereshechenko, V.L. Alperovich, H.E. Scheibler, A.S. Terekhov. e-J. Surf. Sci. Nanotech. **5**, 80 (2007).
[4] U. Weigel, D.A. Orlov, S.N. Kosolobov, D. Schwalm, A.S. Terekhov, A. Wolf. Nucl. Instr. and Meth. A **536**, 323 (2005).
[5] Yu.A. Mamaev, L.G. Gerchikov, Yu.P. Yashin, D.A. Vasiliev, V.V. Kuzmichev, V.M. Ustinov, A.E. Zhukov, V.S. Mikhrin, A.P. Vasiliev. Appl. Phys. Lett. **93**, 081114 (2008).
[6] W.E. Spicer. Appl. Phys. **12**, 115 (1977).
[7] J.W. Schwede, I. Bargatin, D.C. Riley, B.E. Hardin, S.J. Rosenthal, Y. Sun, F. Schmitt, P. Pianetta, R.T. Howe, Z.-X. Shen, N.A. Melosh. Nat. Mater. **9**, 762 (2010).
[8] J.W. Schwede, T. Sarmiento, V.K. Narasimhan, S.J. Rosenthal, D.C. Riley, F. Schmitt, I. Bargatin, K. Sahasrabuddhe, R.T. Howe, J.S. Harris, N.A. Melosh, Z.-X. Shen. Nat. Commun. **4**, 1576 (2013).
[9] J.H. Pollard. Proc. 2nd European Electro-Optics Makets and Technology Conference, p. 316 (1974).

[10] C.A. Sanford, N.C. MacDonald. J. Vac. Sci. Technol. B **8**, 1853 (1990).
[11] Z. Liu, Y. Sun, P. Pianetta, R.F.W. Pease. J. Vac. Sci. Technol. B **23**, 2758 (2005).
[12] D.-I. Lee, Y. Sun, Z. Liu, S. Sun, P. Pianetta. Appl. Phys. Lett. **91**, 192101 (2007).
[13] D.J. Bradley, M.B. Allenson, B.R. Holeman. J. Phys. D: Appl. Phys **10**, *1*, 111 (1977).
[14] D.C. Rodway, D.J. Bradley. J. Phys. D: Appl. Phys. **17**, L137 (1984).
[15] D.A. Orlov, M. Hoppe, U. Weigel, D. Schwalm, A.S. Terekhov, A. Wolf. Appl. Phys. Lett. **78**, *18*, 2721 (2001).
[16] V.V. Bakin, A.A. Pakhnevich, S.N. Kosolobov, H.E. Scheibler, A.S. Jaroshevich, A.S. Terekhov, JETP Lett. **77**, 167 (2003)
[17] V.L. Alperovich, D.M. Kazantsev, A.G. Zhuravlev, L.D. Shvartsman. Appl. Surf. Sci. **561**, 149987 (2021).
[18] A.G. Zhuravlev, A.S. Romanov, V.L. Alperovich. Appl. Phys. Lett. **105**, 251602 (2014).
[19] A.G. Zhuravlev, V.S. Khoroshilov, V.L. Alperovich, JETP Lett. **105**, 686 (2017).
[20] A.G. Zhuravlev, V.S. Khoroshilov, V.L. Alperovich. Appl. Surf. Sci. **483**, 895 (2019).
[21] B. Laikhtman. Phys. Rev. B **46**, 4769 (1992).
[22] A.V. Rodina, A.Yu. Alekseev, Al.L. Efros, M. Rosen, B.K. Meyer. Phys. Rev. B **65**, 125302 (2002).
[23] G. Bastard. Phys. Rev. B **24**, 5693 (1981).
[24] S. Karkare, J. Feng, J. Maxson, H.A. Padmore. Rev. Sci. Instrum. **90**, 053902 (2019).
[25] V.V. Bakin, K.V. Toropetsky, H.E. Scheibler, A.S. Terekhov, L.B. Jones, B.L. Militsyn, T.C.Q. Noakes. Appl. Phys. Lett. **106**, 183501 (2015).
[26] E.L. Nolle. FTT **31**, *11*, 225 (1989) (in Russian).
[27] V.L. Korotkikh, A.L. Musatov, V.D. Shadrin, JETP Lett. **27**, *11*, 652 (1978).
[28] M.G. Burt, J.C. Inkson. J. Phys. D: Appl. Phys. **9**, *1*, 43 (1976).
[29] G. Vergara, A. Herrera-Gómez, W.E. Spicer. Surf. Sci. **436**, 83 (1999).
[30] S. Karkare, I. Bazarov. Appl. Phys. Lett. **98**, 094104 (2011).
[31] F. Stern. Phys. Rev. B **17**, *12*, 5009 (1978).
[32] G.D. Mahan. Phys. Rev. B **2**, *11*, 4334 (1970).
[33] J.B. Pendry. Surf. Sci. **57**, 679 (1976).
[34] L.S. Braginsky, D.A. Romanov. FTT **37**, *7*, 2122 (1995). (in Russian).
[35] J. Olde, G. Mante, H.-P. Barnscheidt, L. Kipp, J.-C. Kuhr, R. Manzke, M. Skibowski, J. Henk, W. Schattke. Phys. Rev. B **41**, *14*, 9958 (1990).

Translated by A.Akhtyamov